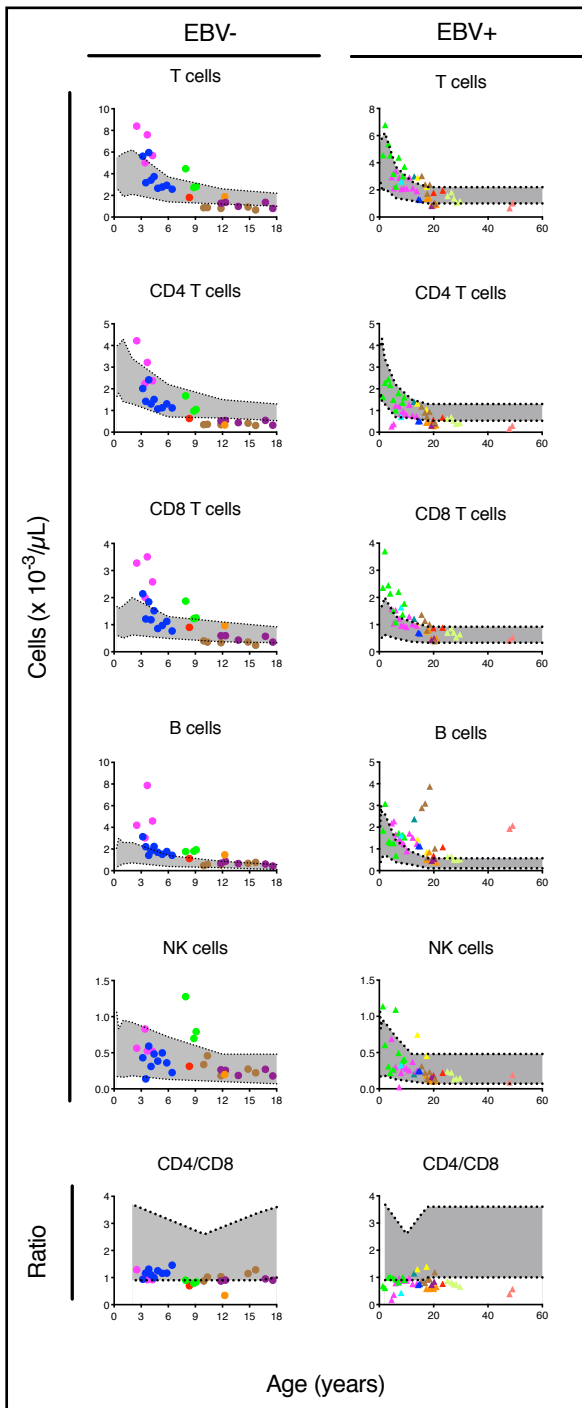
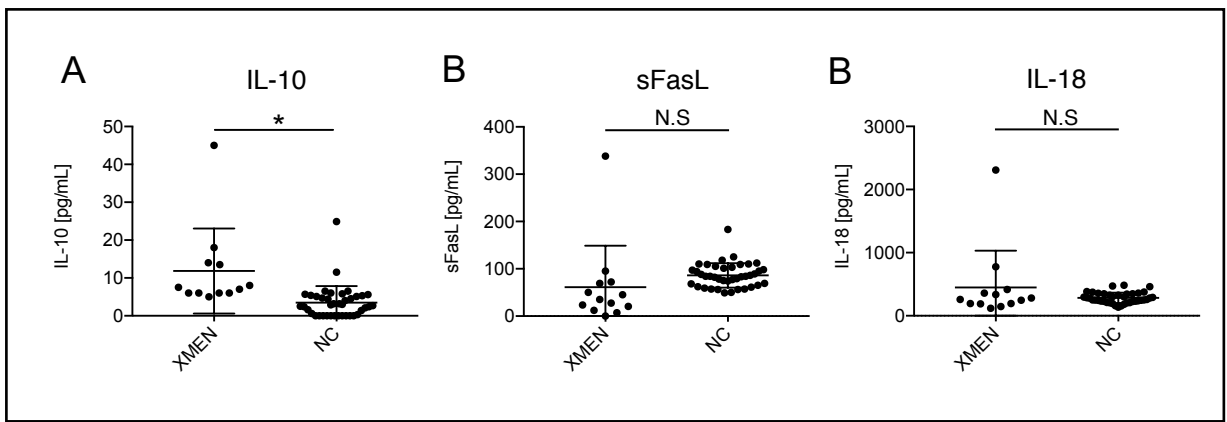
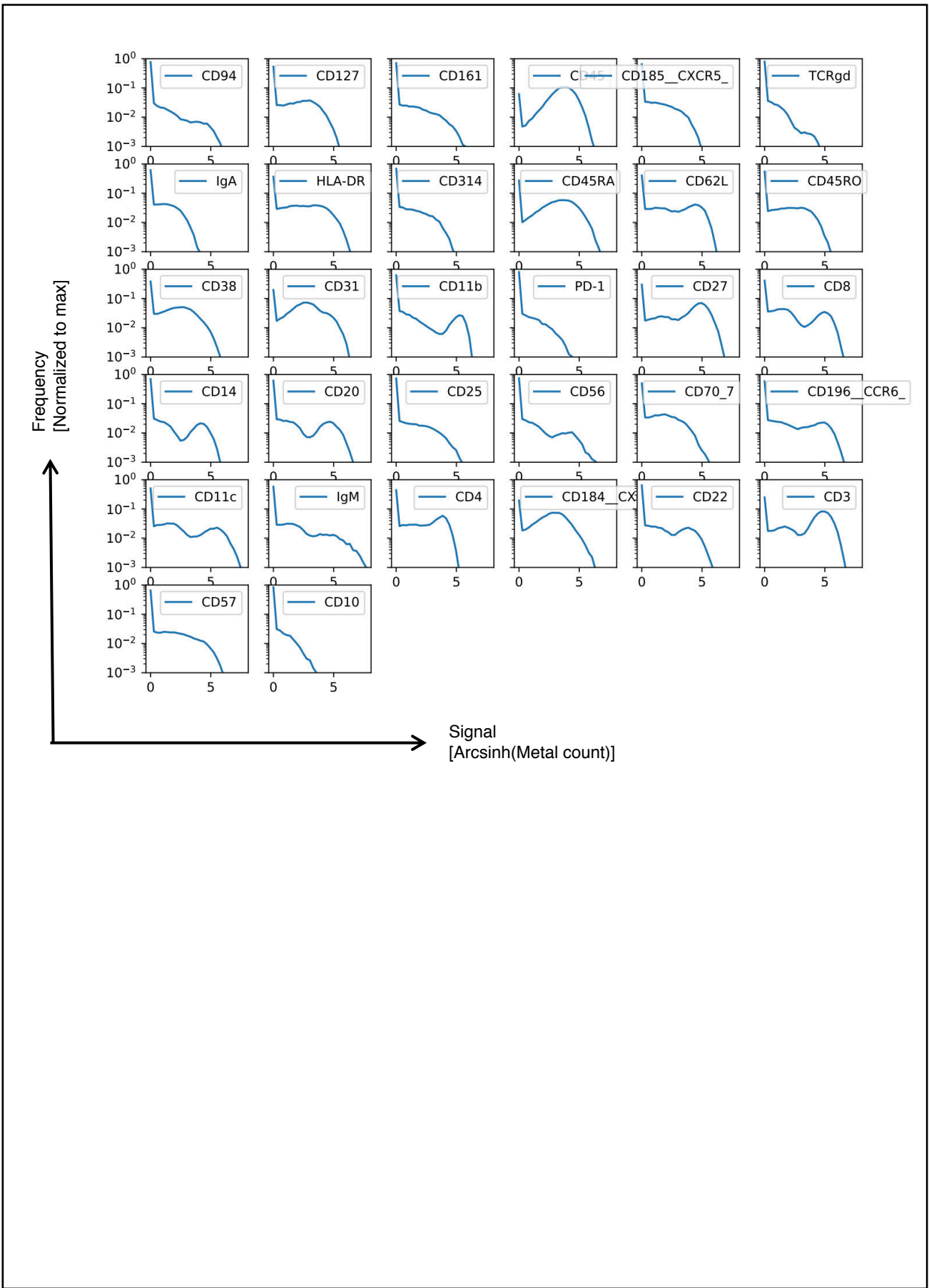


Supplementary figure 1

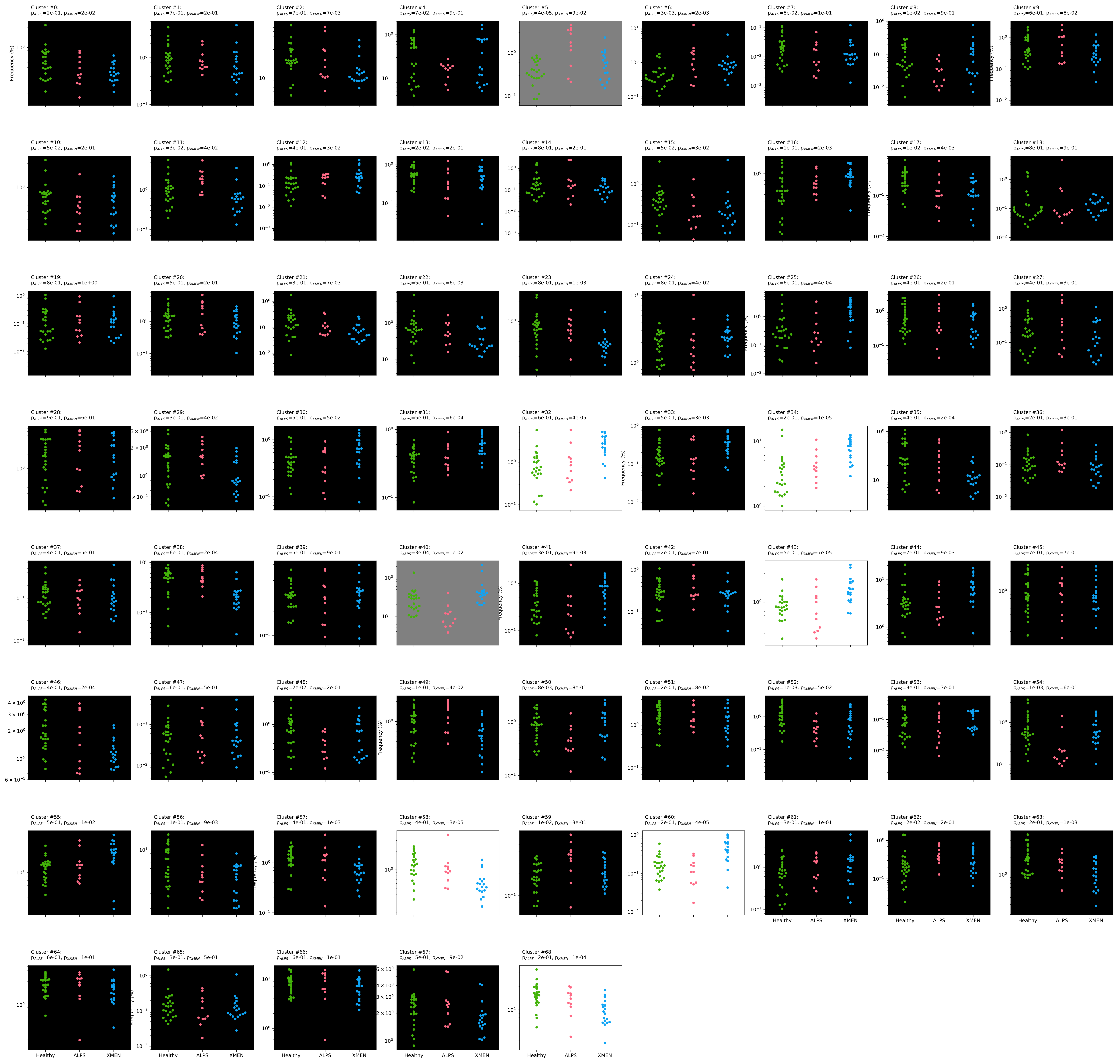


Supplementary figure 2

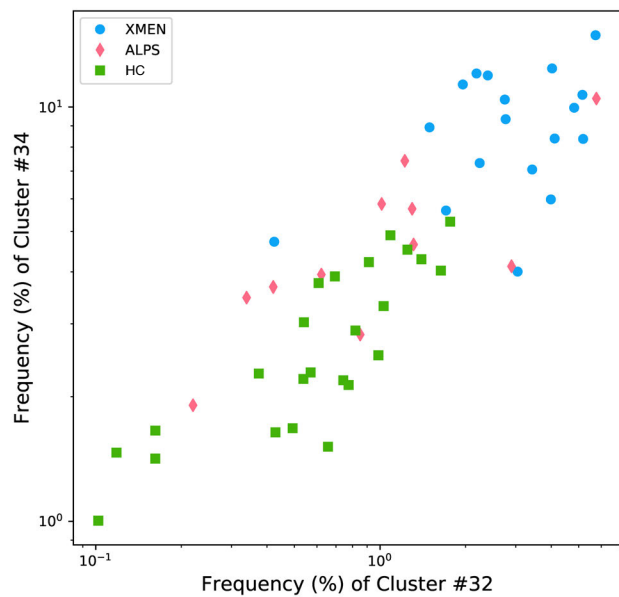




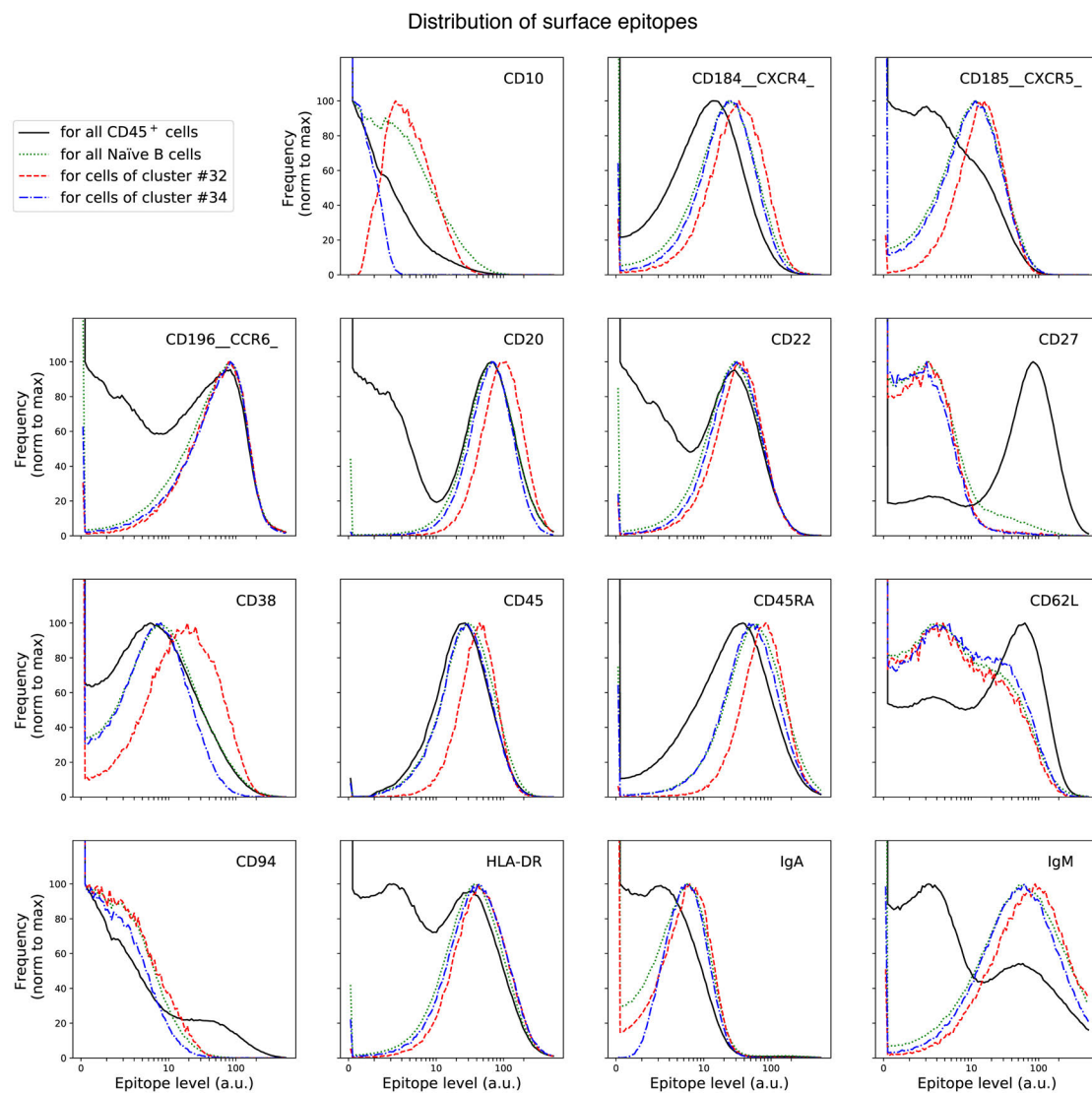
Supplementary figure 4

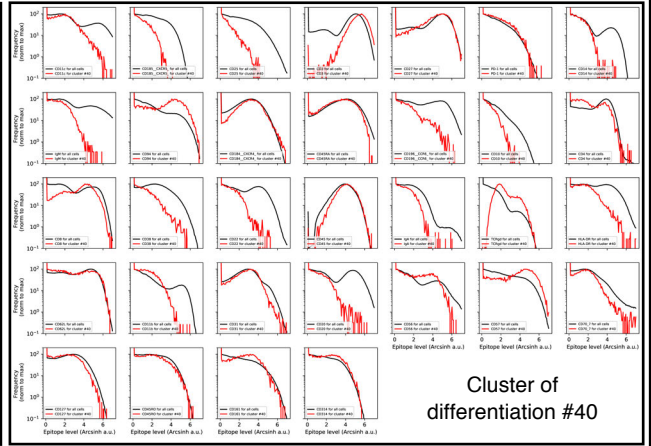
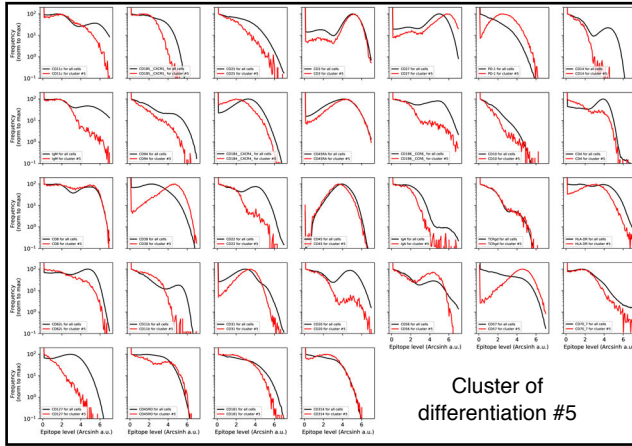
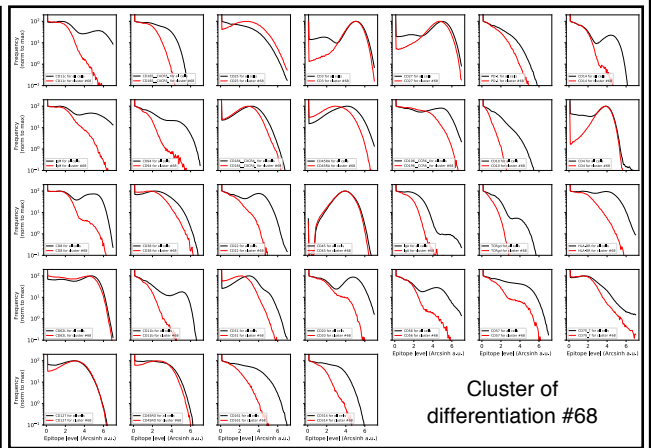
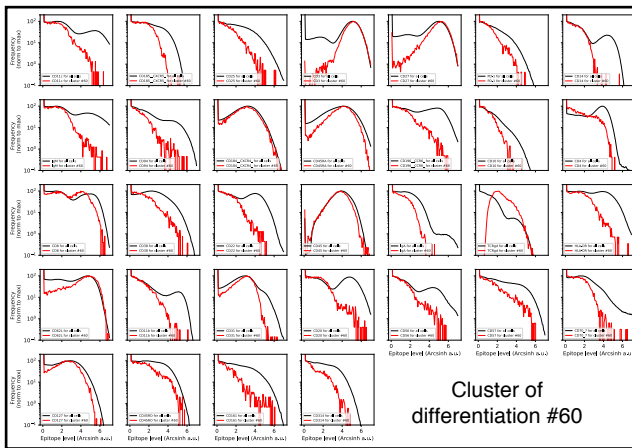
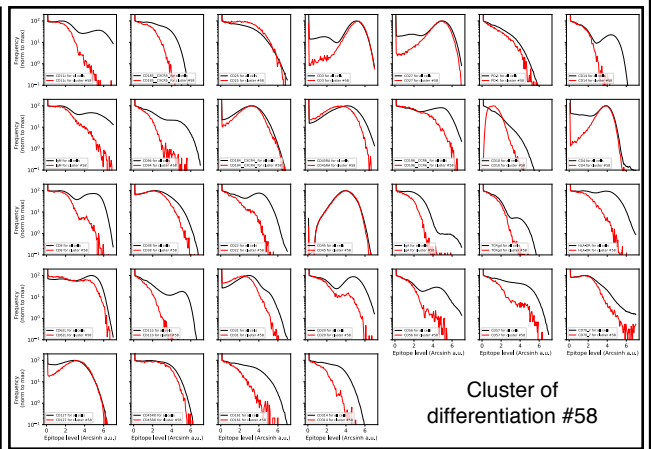
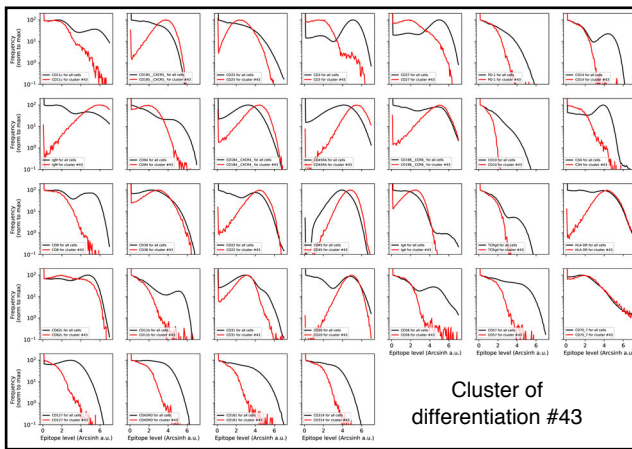


A

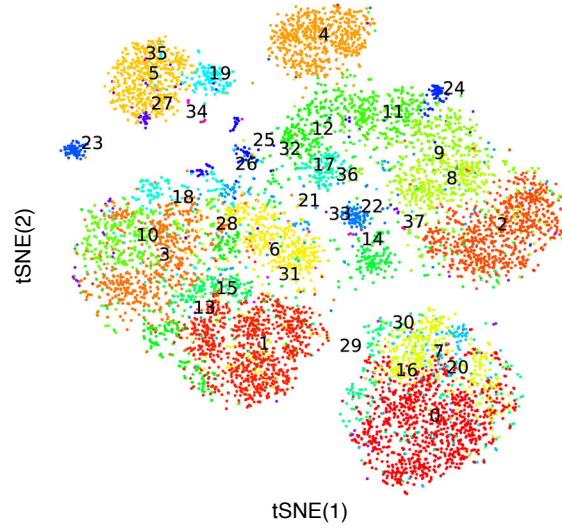


B

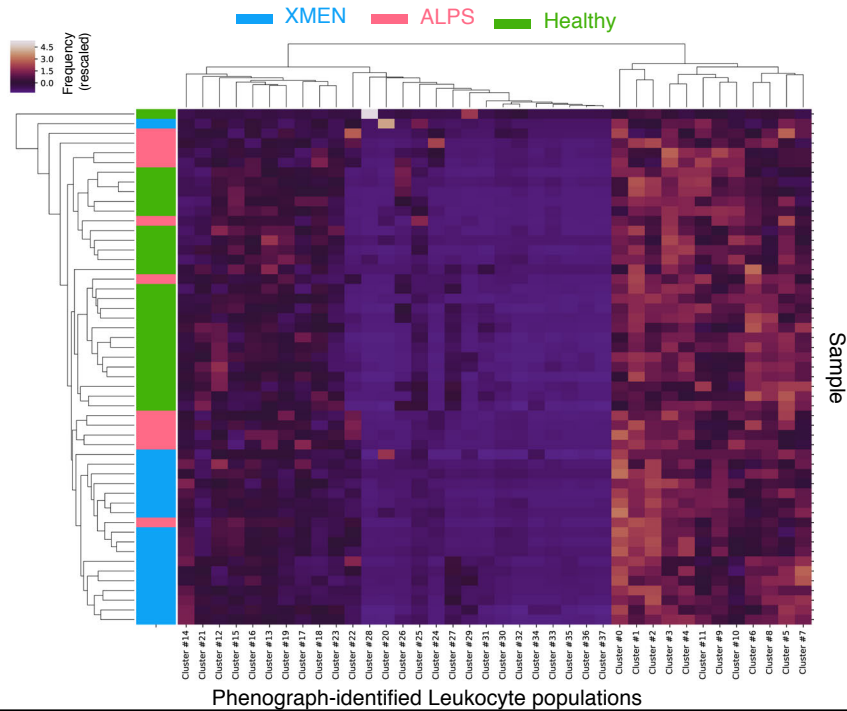


A**B**

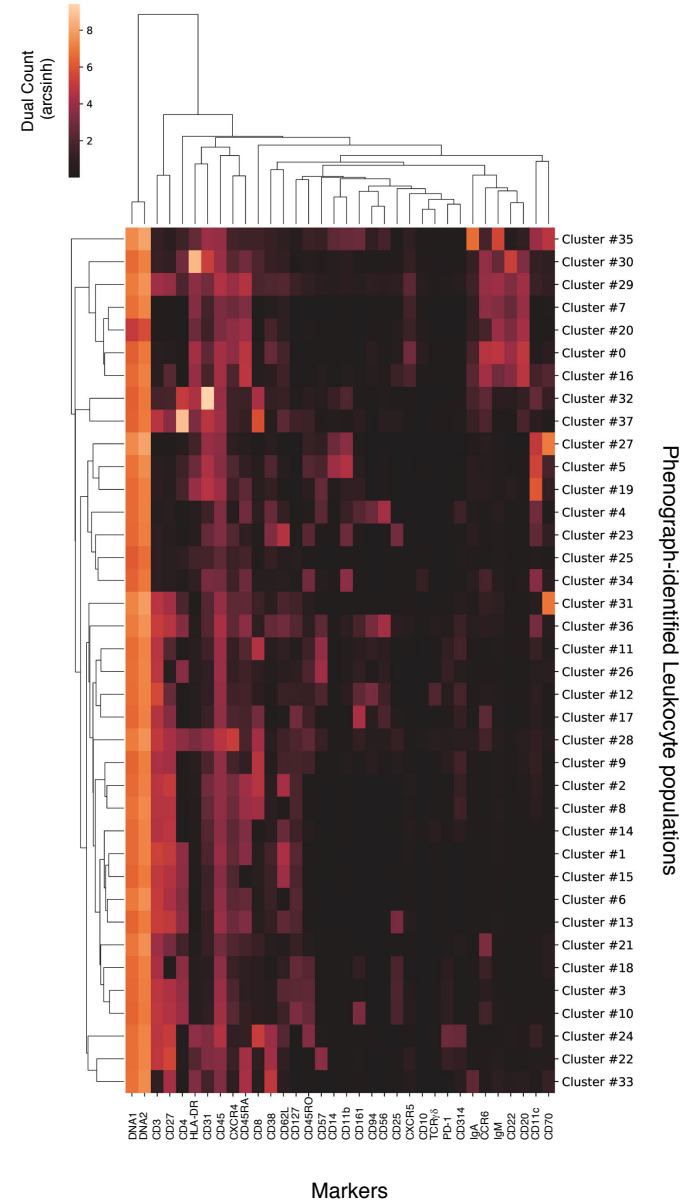
A



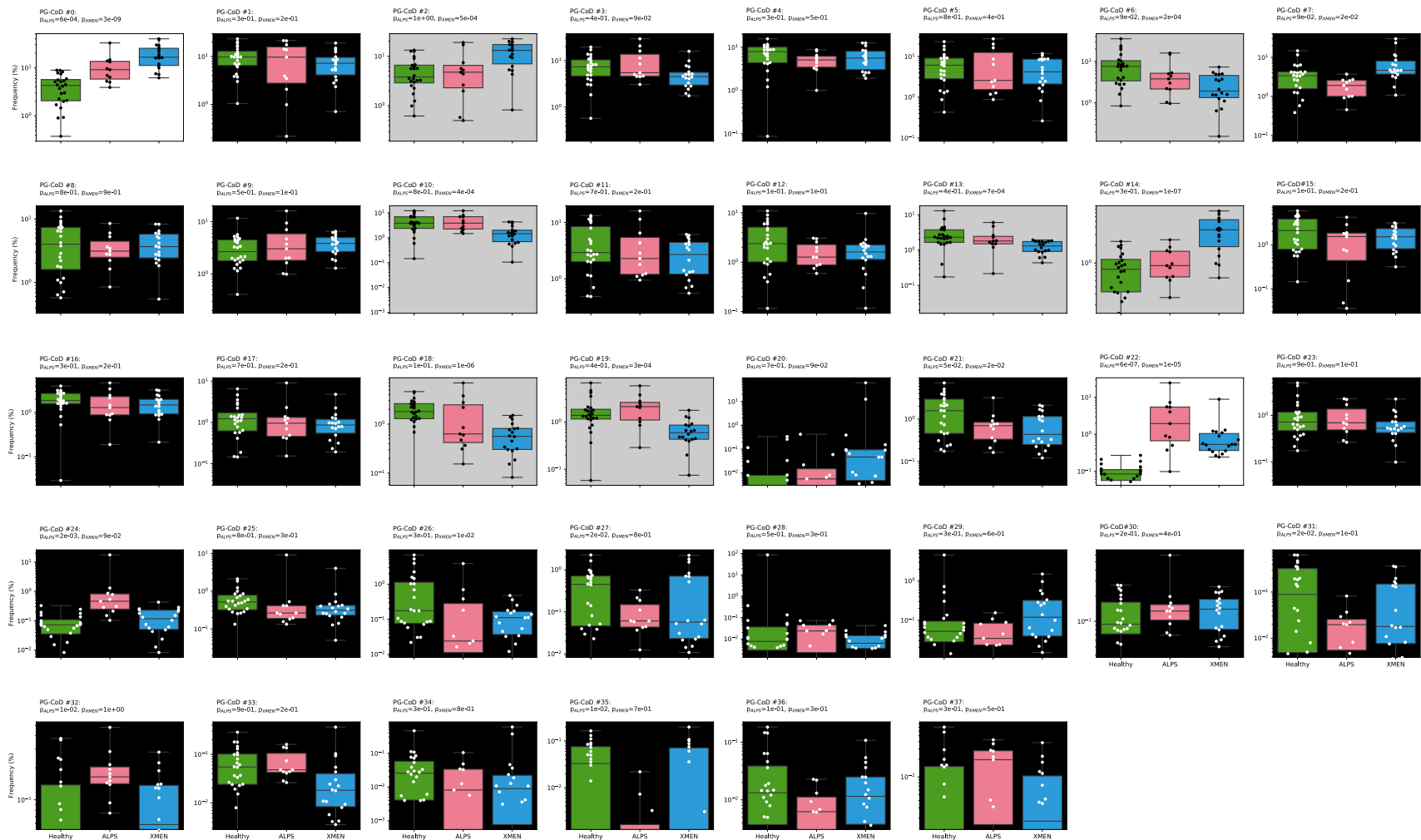
C



B



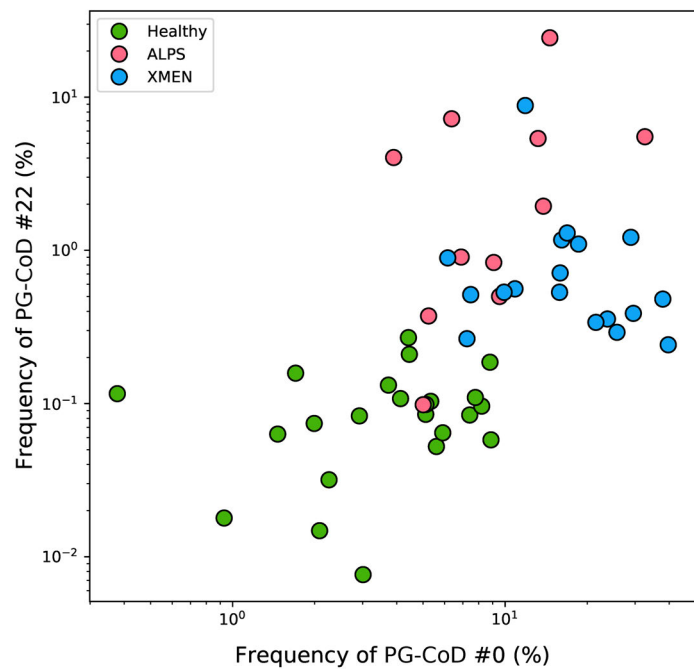
Supplementary Figure 8



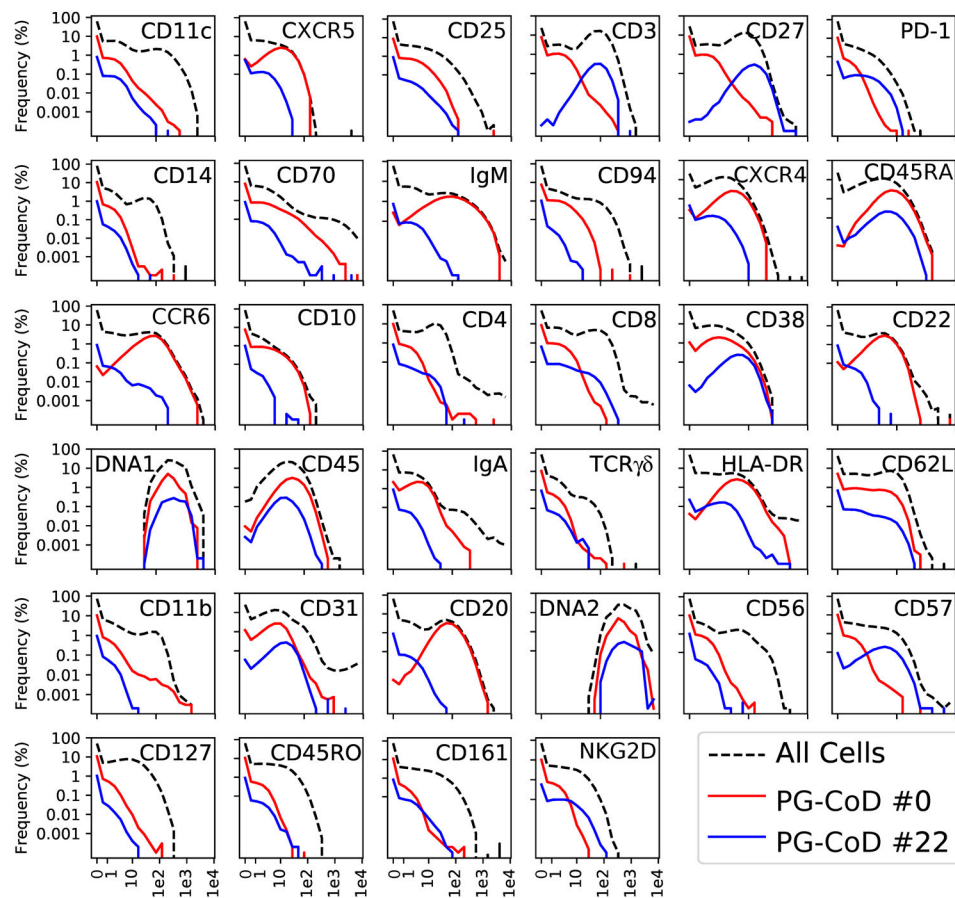
Supplementary Figure 9

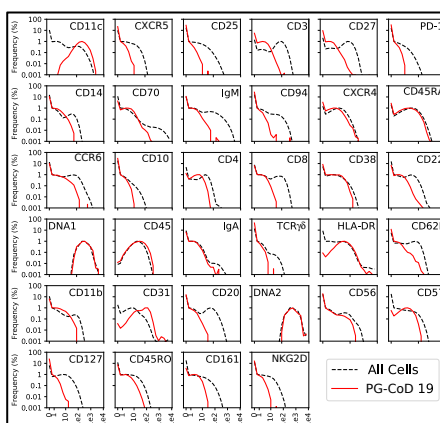
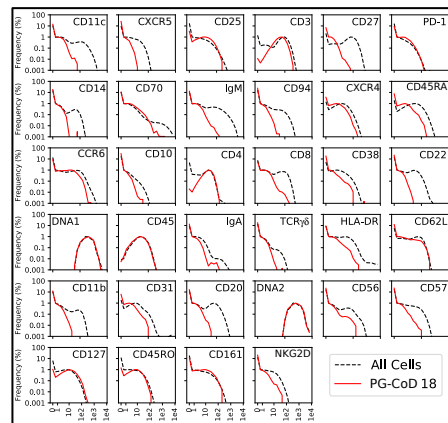
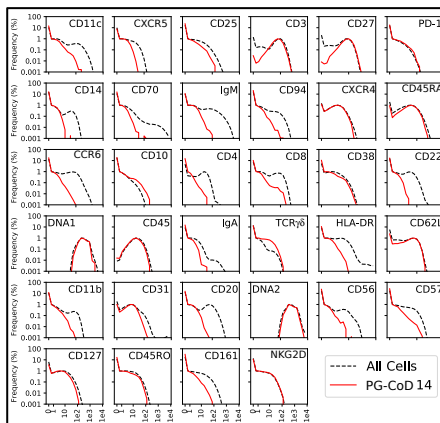
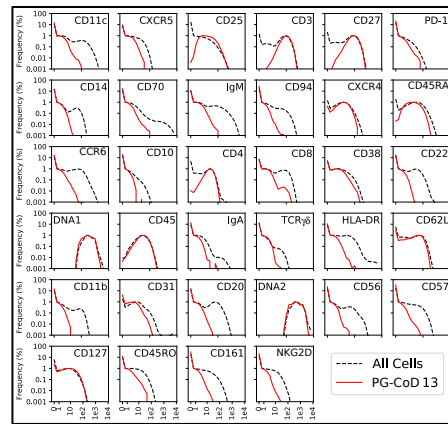
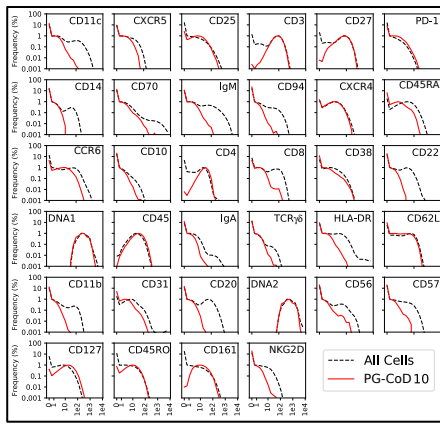
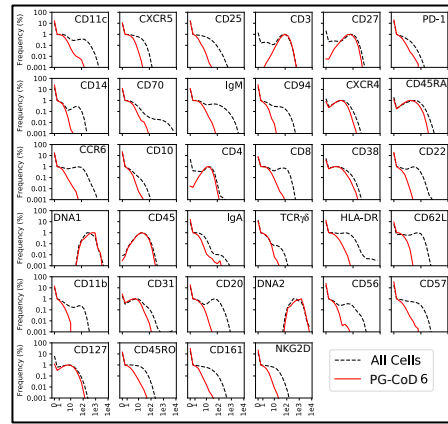
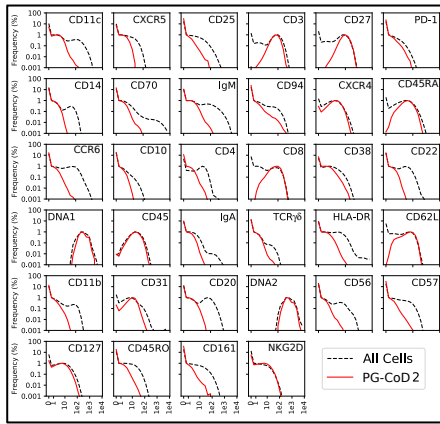
A

B

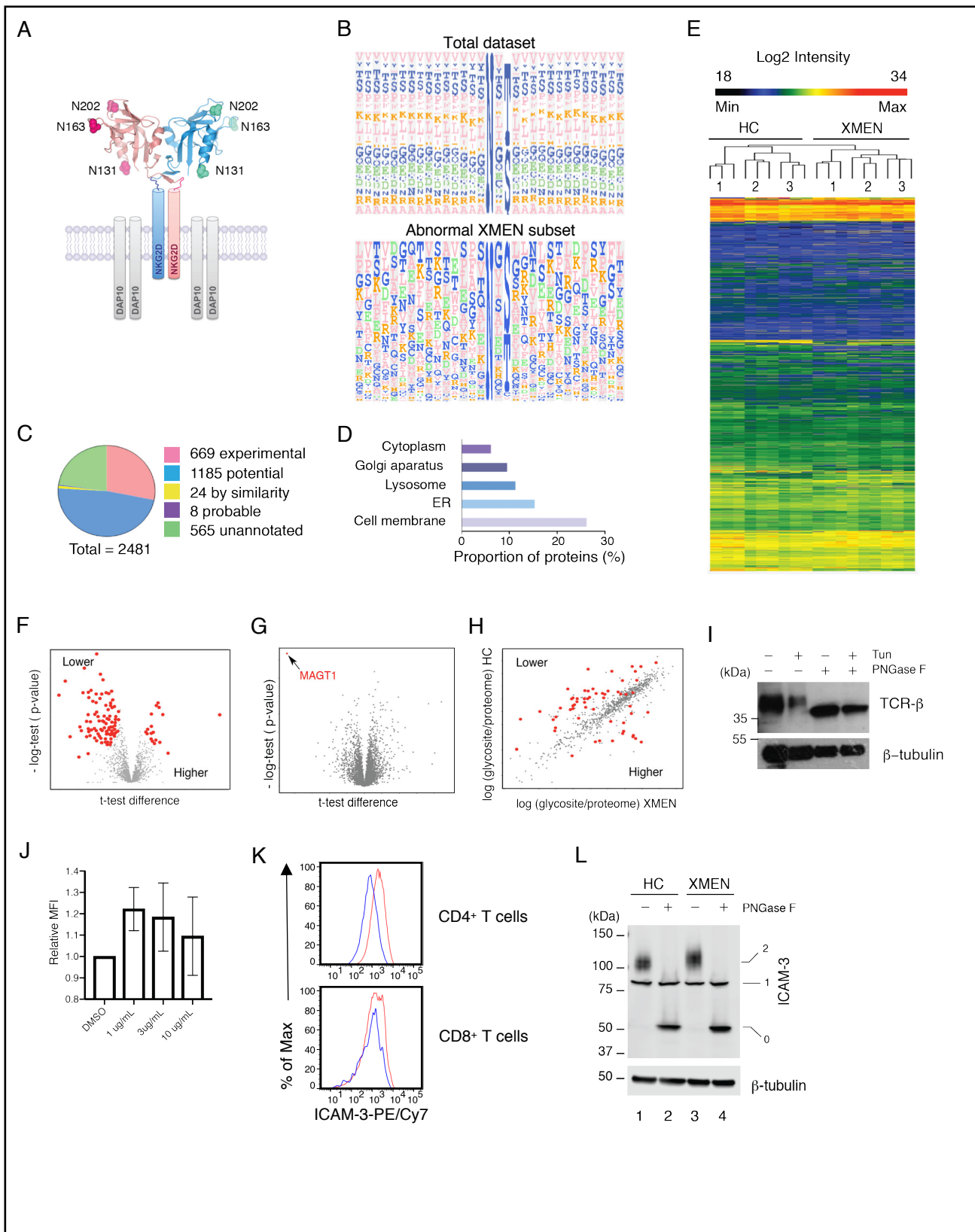


Distribution of surface epitopes

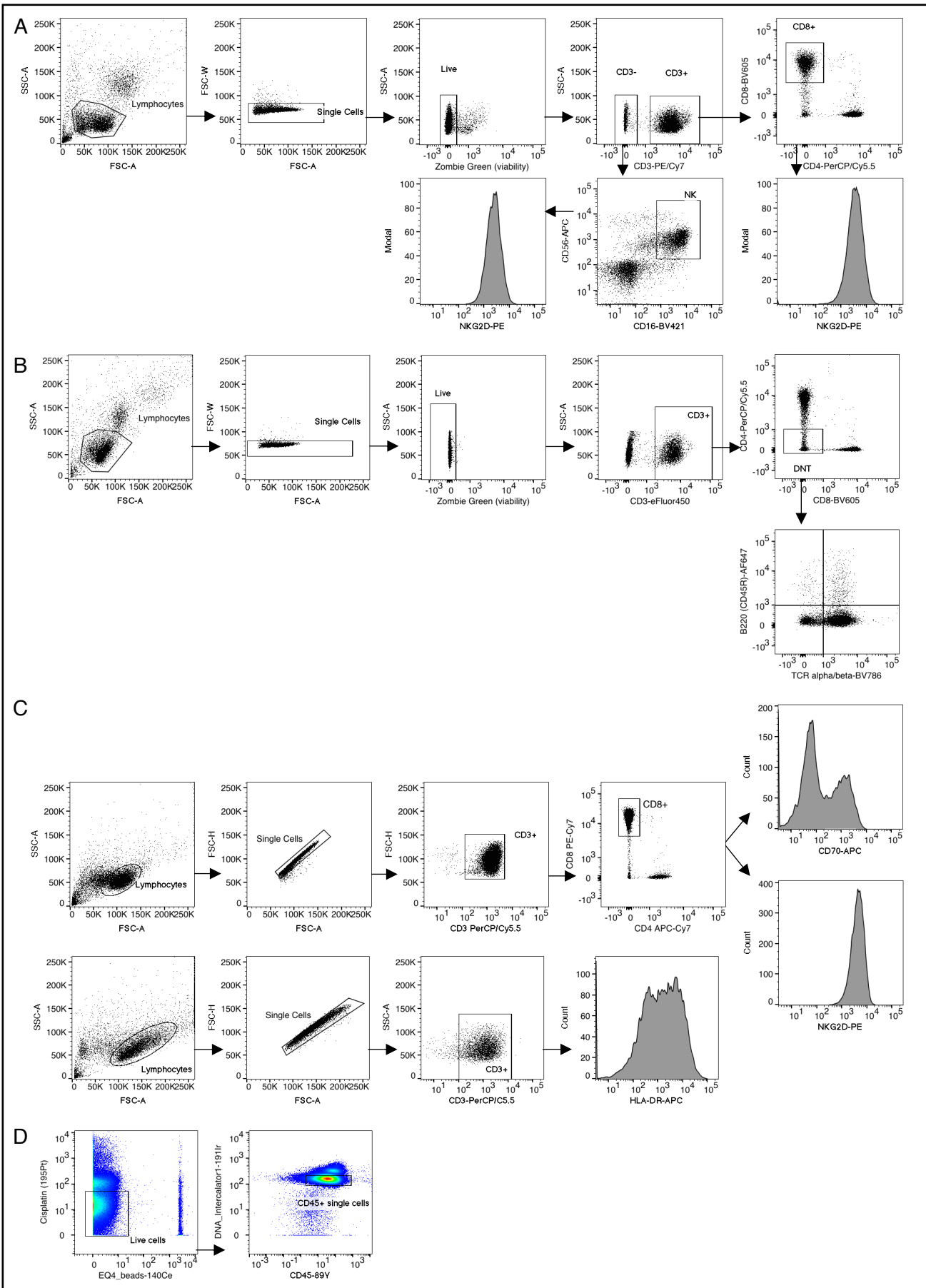




Supplementary figure 11



Supplementary figure 12



Supplementary Figure 1: Imaging and pathological findings in XMEN disease. (A), Quantification of log NKG2D MFI on CD8⁺ T cells (**top**) and CD16⁺CD56⁺ NK cells (**bottom**) of 6 healthy controls (HC), 6 EBV-naïve (EBV-), and 9 EBV-positive (EBV+) XMEN patients. Data are expressed as mean ± standard deviation. **** $P < 0.0001$ by ordinary one-way ANOVA with Tukey's multiple comparisons test. N.S., not statistically significant. (B) Facial molluscum contagiosum lesions (black arrows) in an EBV-naïve patient. (C) CT scan of the chest showing bilateral axillary lymphadenopathy (yellow arrows) in an EBV-infected patient. Contrast-enhanced CT scans showing cervical lymphadenopathy (yellow arrows) in an EBV-naïve (D) and an EBV-infected (E) patient. (F) Contrast-enhanced CT scan showing a large mediastinal lymph node (yellow arrow) in an EBV-naïve patient. (G) CT scan of the brain from same patient shown in figure 1L demonstrating multifocal calcifications (yellow arrows) in the bilateral frontal lobes, thalami, and basal ganglia. (H) FDG PET-CT scan showing a mildly hypermetabolic subcutaneous mass, identified on biopsy as liposarcoma, in the right upper chest wall posteriorly (white arrow). Images (I-N) depict histopathological findings from liver biopsies of EBV-infected patients. (I) Hematoxylin and eosin (HE) stains showing mild portal chronic inflammatory infiltrate, foci of lobular inflammation, and minimal steatosis in EBV-infected patient; (J) focal fatty change and mild periportal fibrosis in liver autopsy of patient deceased from EBV-lymphoproliferative disease; and (K) liver biopsy from patient with persistent EBV viremia depicting moderate steatosis, frequent foci of lobular inflammation, and marked glycogenosis. Reticulin (L) and Masson's trichrome (M) staining of a liver biopsy from same EBV⁺ XMEN patient showing prominent ballooning injury and bridging fibrosis. (N) Numerous Mallory bodies are evident by immunoperoxidase staining for ubiquitin.

Supplementary Figure 2: Lymphocyte subsets in EBV-naïve and EBV-infected XMEN patients: Lymphocyte immunophenotyping of peripheral blood cells from 7 EBV-naïve (-) and 12 EBV-infected (+) XMEN patients is shown according to age. Normal ranges for age are shown in gray and represent the 10th to 90th percentiles based on published data(1). Patients are listed according to their assigned family letter, followed by their patient number: EBV-naïve (●): H.1, J.1, J.2, L.1, L.2, M.1, M.2; and EBV-infected (▲): A.1, A.2, D.1, E.1, G.1, G.2, L.2, M.1*, N.1, and O.1. *Refers to values after developing EBV infection.

Supplementary Figure 3: ALPS biomarkers in XMEN disease. Comparison of serum IL-10 (A), sFasL (B), and IL-18 (C) levels in pg/mL between 13 XMEN patients and 40 normal controls (NC). For individuals with >1 determination, a median value is shown. * $P < 0.05$ by mixed model analysis. N.S. not statistically significant.

Supplementary Figure 4: CyTOF signals for markers. Smoothed densities of signal expression (Arcsin-transformed) versus frequency of 32 lineage markers as indicated.

Supplementary Figure 5: Comparison of the relative abundance of 69 clusters of differentiation between HC, ALPS, and XMEN. Bonferroni-corrected t-test analysis for each of the 69 (0-68) clusters of differentiation identified comparing the corresponding relative abundance of cells from HC (green), ALPS patients (magenta), and XMEN patients (blue). A white background is used for clusters for which there is a statistically significant difference between XMEN and both HC and ALPS; a gray background for those with a statistically significant difference between ALPS and both HC and XMEN. A black background is used for

clusters with no statistically significant difference between samples. The respective *P* value for comparisons between either ALPS or XMEN with healthy controls are shown for each cluster.

Supplementary Figure 6: Distinct clusters of differentiation for XMEN patients. (A) Frequency of cluster of differentiation (CoD) # 32 on the X axis and CoD #34 on the Y axis for XMEN (blue), ALPS (magenta), and healthy controls (HC) (green). **(B)** Histograms for surface marker expression as indicated in all lymphocytes (CD45⁺), all naïve B-cells (CD20⁺CD27⁻), CoD #32, and CoD #34 are shown in black, green, red, and blue, respectively.

Supplementary Figure 7: Cell markers for statistically different clusters of differentiation. Histograms for surface marker expression as indicated in all peripheral blood mononuclear cells (black) and within the respective cluster of differentiation (CoD) (red). **(A)** Cell markers for CoD where ALPS samples were statistically different from both XMEN and HC (CoD #5 and #40). **(B)** Cell markers for four of the CoD where XMEN samples were statistically different from both ALPS and HC (CoD #43, #58, #60, and #68). The “all cells” group is the same for all panels.

Supplementary Figure 8: High-dimensional clustering analysis of mass spectrometry data using Phenograph confirms distinctive immune subsets for XMEN compared to healthy controls and ALPS. (A) Two-dimensional projection of the 38 Phenograph-identified clusters of differentiation (PG-CoD) on CyTOF data acquired from PBMCs of XMEN (n=18), ALPS (n=11), and healthy controls (n=24) as visualized by t-SNE. **(B)** Dendrogram showing these PG-CoD based on their abundance of surface epitopes. **(C)** Dendrogram for the frequencies of these PG-CoD based on unsupervised grouping showing the clustering of XMEN patients (blue), ALPS patients (magenta), and healthy controls (green). Each row refers to one individual sample.

Supplementary Figure 9: Comparison of the relative abundance of 38 Phenograph-identified clusters of differentiation (PG-CoD) between HC, ALPS, and XMEN. Bonferroni-corrected t-test analysis for each of the 38 (0-37) clusters of differentiation identified by Phenograph, comparing the corresponding relative abundance of cells from HC (green), ALPS patients (magenta), and XMEN patients (blue). A white background is used for clusters for which there is a statistically significant difference for both XMEN and ALPS compared with HC; a gray background for those with a statistically significant difference only between XMEN and HC. A black background is used for clusters with no statistically significant difference between samples. The respective *p* value (9e-4 cutoff) for comparisons between CoD frequencies for either ALPS or XMEN compared with healthy controls are shown for each cluster.

Supplementary Figure 10: Distinct Phenograph-identified clusters of differentiation (PG-CoD) for XMEN patients. (A) Frequency of PG-CoD # 0 on the X axis and PG-CoD #22 on the Y axis for XMEN (blue), ALPS (magenta), and healthy controls (HC) (green). **(B)** Histograms for surface marker expression as indicated in all cells, PG-CoD #0 and PG-CoD #22 are shown in black, red, and blue, respectively.

Supplementary Figure 11: Cell markers for statistically different Phenograph-identified clusters of differentiation (PG-CoD). Histograms for surface marker expression as indicated in all peripheral blood mononuclear cells (black) and within the respective cluster PG-CoDo (red). The “all cells” group is the same for all panels.

Supplementary Figure 12: Selective glycosylation defects in lymphocytes from patients with XMEN disease. (A) Schematic of NKG2D and its co-receptor DAP10 with the predicted stoichiometry and NLG sites. (B) Motif analysis of the collated NxS/T glycosites identified from glycoproteomics analysis for the complete dataset (**top**) and proteins differentially glycosylated between healthy controls (HC) and XMEN (**bottom**). The height of each symbol indicates relative frequency of each amino acid at that position. (C) Annotation of these proteins in proteomic databases. (D) The cellular location of the proteins from which the peptides were derived. (E) Unsupervised heat map of the entire N-linked glycoproteome analysis of 3 HC and 3 XMEN patients. (F) Volcano plot of the log test *P* value (Y axis) vs. the t-test difference (X axis) of glycopeptide abundance (F) and protein abundance (G) with MAGT1 labelled (red). (H) Log (glycosite/proteome) for HC (Y axis) vs. XMEN (X axis) showing underglycosylated proteins to the upper left (Lower) and overglycosylated proteins to the lower right (Higher). (I) Immunoblot of TCR- β and β -tubulin in T cells with (+) or without (-) PNGase F treatment after incubation with (+) or without (-) 10 μ g/ml tunicamycin (Tun) for 48 hours. (J) Flow cytometry analysis showing mean fluorescent intensity (MFI) quantification of TCR- β on T cells treated with tunicamycin for 48 hours relative to the DMSO-treated control. (K) Flow cytometry histogram of ICAM-3 on CD4⁺ (**top**) and CD8⁺ (**bottom**) T cells from HC (blue) and XMEN (red). (L) Immunoblot of ICAM-3 and β -tubulin in T cells from HC and XMEN. Fully-glycosylated (2), non-specific (1), and unglycosylated (0) bands are indicated. Results shown in (I), (K), and (L) are representative of three independent repeats.

Supplementary Figure 13: Flow and mass cytometry gating strategies. (A) Flow cytometry gating strategy to select CD3⁺ T cells, CD3⁺CD8⁺ T cells, and CD16⁺CD56⁺ NK cells from peripheral blood mononuclear cells (PBMCs). Histograms showing the mean fluorescent intensity (MFI) for NKG2D on gated CD8⁺ T cells and CD16⁺CD56⁺ NK cells are shown. A variation of this gating strategy was used to evaluate surface expression of ICAM3 on CD4⁺ and CD8⁺ T cells. (B) Flow cytometry gating strategy to select CD4⁻CD8⁻ DNT cells, TCR $\alpha\beta$ ⁺ DNT cells, and B220⁺TCR $\alpha\beta$ ⁺DNT cells from PBMCs. (C) Flow cytometry gating strategy to determine the MFI of CD70 and NKG2D from CD8⁺ T cell blasts (**top**) and HLA-DR from CD3⁺ T cells (**bottom**). A similar gating strategy or variations of that was used to assess surface expression of CD5, CD28, and TCR $\alpha\beta$ on T cell blasts (not shown). (D) Gating strategy for mass cytometry.

References

1. Shearer WT, Rosenblatt HM, Gelman RS, Oyomopito R, Plaeger S, Stiehm ER, et al. Lymphocyte subsets in healthy children from birth through 18 years of age: the Pediatric AIDS Clinical Trials Group P1009 study. *J Allergy Clin Immunol.* 2003;112(5):973-80.

Supplementary Table 1: XMEN Patients with clinical and laboratory features

Clinical manifestations	Patients	Frequency
Recurrent ear and sinopulmonary infections	A.1, A.2, A.3, G.1, I.2, J.1, J.2, L.1, L.2, M.1, M.2 , N.1, O.1, P.1 , Q.1, R.1	70% (16/23)
Chronic lymphadenopathy	A.1, A.3, B.1*, D.1, E.1, G.1, G.2, H.1, J.2 , K.2, M.1, M.2 , N.1, P.1 , R.1	65% (15/23)
Splenomegaly	A.1, B.1*, D.1, E.1, G.2, K.1, K.2, P.1 , R.1	39% (9/23)
Lymphoma/LPD	B.1, D.1, E.1, I.2, K.2, M.2 , N.1, P.1 †, R.1	39% (9/23)
Molluscum contagiosum	A.2, E.1, K.1, K.2, L.1, L.2, M.1, M.2	35% (8/23)
Recurrent mouth sores	G.1, G.2, I.2, J.2 , K.1, K.2, L.1, M.2	35% (8/23)
Severe autoimmune cytopenias (grade 4)	A.1, D.1, H.1 , I.2, K.1, N.1, O.1, R.1	35% (8/23)
Skin Warts or Condylomata acuminata	A.1, A.3, E.1, G.1, J.2, M.2 , O.1	30% (7/23)
Guillain-Barré syndrome	B.1*, M.2 , N.1, R.1	17% (4/23)
HSV infection	A.1, A.2, E.1‡, N.1	13% (3/23)
Other autoimmune	A.1 (alopecia partialis), J.1 (episcleritis), R.1 (Autoimmune hepatitis (1))	13% (3/23)
Pericardial and/or pulmonary effusions	B.1, N.1	9% (2/23)
EBV-negative malignancy	I.2	4% (1/23)
Laboratory and imaging findings		
Transient elevation of liver enzymes	A.1, A.2, A.3, B.1*, D.1, E.1, G.1, G.2, H.1 , I.2, J.1, J.2 , K.1, K.2, L.1, L.2, M.1, M.2 , N.1, O.1, P.1 , Q.1, R.1	100% (23/23) ¶
Low NKG2D surface expression on NK and CD8 T cells	A.1, A.2, A.3, B.1, D.1, E.1, G.1, G.2, H.1 , I.2, J.1, J.2 , K.1, K.2, L.1, L.2, M.1, M.2 , N.1, O.1, P.1 , Q.1, R.1	100% (23/23)
Elevated B cells	A.1, A.2, A.3, D.1, E.1, G.1, G.2, H.1 , I.2, J.1, J.2 , K.1, K.2, L.1, L.2, M.1, M.2 , N.1, O.1, P.1 , Q.1, R.1	95% (22/23)
Elevated $\alpha\beta$ DNT cells	A.1, A.2, A.3, D.1, E.1, G.1, G.2, H.1, J.1, J.2 , K.1, K.2, L.1, L.2, M.1, M.2 , O.1, P.1 , R.1	95% (19/20)

Low IgA	A.1, A.2, A.3, D.1, E.1, G.1, G.2, I.2, J.1, J.2, K.1, K.2, L.2, M.1, M.2, N.1, O.1, P.1	78% (18/23)
Low CD4/CD8 ratio	A.1, A.2, A.3, D.1, E.1, G.1, H.1§, I.2, J.1, J.2, K.1, K.2, L.1, L.2, M.1, M.2, N.1, R.1	78% (18/23)
Low IgG	A.1, A.2, A.3, D.1, E.1, I.2, J.1, J.2, K.1, K.2, L.1, L.2, M.1, M.2, N.1, O.1, P.1	74% (17/23)
Persistently elevated EBV-viremia	A.1, A.2, A.3, B.1, D.1, E.1, G.1, G.2, I.2, K.1, K.2, M.1#, M.2#, N.1, O.1, Q.1, R.1	74% (17/23)
Thrombocytopenia	A.1, A.2, B.1*, D.1, E.1, H.1, I.2, K.1, K.2, L.2, M.1, M.2, N.1, O.1, P.1, R.1	70% (16/23)
Transient neutropenia	A.1, A.2, B.1*, D.1, E.1, H.1, I.2, K.1, K.2, L.1, M.1, M.2, N.1, P.1	61% (14/23)
Transient elevations of CPK	A.1, A.2, E.1, G.1, G.2, I.2, J.1, J.2, M.1, M.2, O.1	52% (11/21)
Cave septum pellucidum	A.1, A.2, E.1, D.1	50% (4/8)
CD4 lymphopenia	A.1, A.2, B.1*, E.1, L.1, M.1, M.2, O.1, P.1, R.1	44% (10/23)
Central nervous system abnormalities	B.1 and N.1 (brain atrophy greater than expected for age), E.1 (small areas of brain leukomalacia and gliosis consistent with history of PRES), Q.1 (cerebrum, cerebellum, brainstem, and spinal atrophy with calcifications in the basal ganglia and thalami)	17% (4/23)

EBV-naïve and EBV-infected patients are shown in red and black respectively. Patients in blue were followed for several years before and after EBV-infection. * In the setting of acute lymphoma. † EBER-negative mediastinal mass comprised of atypical lymphohistiocytic proliferation of uncertain malignant potential. ‡ Due to chemotherapy, not accounted for frequency determination. § Variable. ¶ One patient (P.1) had elevated liver enzymes only once out of multiple determinations. # EBV-naïve at time of XMEN diagnosis. PRES: Posterior reversible encephalopathy syndrome.

Supplementary table 2: Laboratory results

Patient	A.1	A.2	A.3	B.1††	D.1	E.1	G.1	G.2	H.1	I.2	J.1	J.2	K.1	K.2	L.1	L.2	M.1	M.2	N.1	O.1	P.1	Q.1	R.1	
Hemoglobin (g/dL)	10.9-14.8	11.2-14.6	12.9	9.7¶	3.7-13.4	13-15	12.9-14	13.9-14.9	4.4-13.6	11-17.2	11.1-12.8	11.9-14.3	4.8-13.9	13.8-14.3	11.3-13.2	11-14.2	13.1-14.1	12.9-13.9	3.1-12.5	14.2-15.4	8.5-13.5	14.6-16.8	3.2**	
Platelet count (161-347 K/uL)	47-436	111-386	164	7-111†	133-205	88-147	226-233	174-276	108-400	38-92	224-304	221-276	33-169	116-137	214-286	179-368	140-190	111-150	4-316	168-233	111-939	186-210	5**	
Neutrophils absolute (K/uL)	0.41-36.33	0.5-4.13	3.24	4.2¶	1.15-3.47	1.31-2.74	3.14-3.19	2.94-3.85	0.79-3.13	1.18-2.26	2.45-4.09		0.1-5.2	1.55-3.16	1.26-5.59	1.54-7.69	1.31-3.43	1.31-2.15	0.71-12.87	1.84-2.9	0.2-10.9	1.95-2.16	2.5-6.5	
CD4/CD8 (1.11-5.17)	0.17-1.1	0.82-1.13	1.03	3.7-8.5†	0.86-1.24	0.54-0.71	0.66-0.77	1.3-1.4	0.94-1.46	0.69-0.84	0.92-1.29	0.79-1.02	0.44	0.73	0.34-0.36	0.79-1.02	0.73-0.95	0.87-1.29	0.57	1.7	1.7	1.18	0.39-0.72	
T cells (cells/uL)	1253-3389	1562-6786	1468	175-318†	1245-3028	695-1405	1792-1955	2244-2911	2578-5618	524-1900	5010-8397	1266-4461	2633	1264-1308	1399-2104	10900-1955	724-1351	665-927	648-1126	3000	1,158	1963	897-2000	
CD4 T cells (cells/uL)	272-1309	741-2443	655	138-277†	521-1190	244-459	577-683	1047-1326	1070-2416	202-710	2249-4218	501-1675	711	509-514	280-364	412-734	296-520	310-415	162-394	1401	674	1004	351-543	
CD8 T cells (cells/uL)	545-1580	653-3706	637	25-37†	581-1364	380-794	870-889	749-1016	767-2141	273-868	2002-3505	564-1870	1635	676-702	725-1048	488-909	358-596	241-401	416-674	1215	395	878	490-1380	
B cells (cells/uL)	688-2279	717-1727	1307	40-74†	502-4088	369-709	692-1086	852-1448	1420-3138	375-758	3025-7869	1214-1928	1635	1136	1182-1553	901-1286	360-862	468-767	745-2073	2106-2321	952	2716	890-1776	
NK cells (cells/uL)	155-689	144-1139	209	2-23†	98-355	60-196	187-222	454-747	138-498	50-302	520-845	122-1277	328	244	118-377	142-313	155-264	182-458	89-486	203	222	291	140-240	
NKT cells (cells/uL)	31-255	89-402	263	5†	46-268	27-134	312-540	229-288	50-558	41-87	291-726	76-340	92	96	250-401	134-369	30-136	23-34	144	N/A		N/A	N/A	
CD4+CD45RA+CD31+ T cells (cells/uL and %)	310 (10.5%)	978 (17.4%)	233 (7.8%)	N/A	N/A	57-80 (4.1-4.7%)	95 (2.9%)	178 (5%)	714 (14.9)	N/A	1312-1880 (11.8-15.2%)	89-199 (2.8-3.6%)	208 (4.5%)	190 (7.1%)	53-65 (1.5-2.1%)	260-292 (8.1-10.3%)	138-200 (11.1-11.6)	N/A	N/A	N/A	N/A		6.80%	N/A
αβDNT cells (cells/uL and %)			90 (3%)	N/A	151 (3.2%)	34-42 (1.9-2.5%)	186 (5.7%)	85 (2.4%)	880-1089 (8.2-13.8%)	N/A	488-542 (3.4-5.6%)	537-1295* (3.6%)	120 (2.6%)	38 (1.4%)	84-104 (2.6-2.9%)	44-56 (1.5-1.8%)	31-45 (2.5-2.9%)	N/A	N/A	40 (1.3%)	69 (4.2%)	1.10%	32 (3.2%)	
IgG (716-1711 mg/dL)	654-2460*	277-1450*	452	734	427-1690*	525-927*	1297-1401	1069-1264	902-1161	387-2240*	563-868*	537-1295*	570	334-540	543-608	759-1188	490-1052	752-960	518-691*	656-1338*	529-796*	776-952	880-1650	
IgA (47-249 mg/dL)	47-165	<7-16	106	128	33-84	35-54	59-61	40-59	26-62	22-42	16-23	32-48	30	64-73	70-76	20-29	31-52	29-45	26-33	56-73	23	82-105	50-75	
IgM (15-188 mg/dL)	52-150	22-94	31	14	43-89	51-86	135-170	207-241	137-206	27-63	11-20	187-265	119	159-167	95-114	87-97	169-244	250-369	20-36	105-151	83	133-181	52-145	
EBV PCR (Log10 IU/mL)	4.29-5.85	<2.40-5.28	3.33	Positive	<2.4-3.98	3.48-5.34	3.87-4.17	4.24-4.31	Negative	4.08-4.82	Negative	Negative	4.16	4.85-5.47	Negative	Negative	Negative	Negative	2.91-3.69	5.92†	Negative	3.58	Positive	
CMV PCR (10 ⁶ copies/mL)	Negative	Negative	Negative	Negative	Negative	Negative	Negative	Negative	Negative	Negative	Negative	Negative	Negative	Negative	Negative	Negative	Negative	Negative	Negative	Negative	Negative	Negative	150-600†	
ALT (5-30 U/L)	30-141	24-71	60	79¶	32-204	26-104	36-49	26-137	22-61	45-380	29-53	55-171	148	28-33	22-190	24-47	23-95	34-74	27-35	40-531	11-84	85-137	418	
AST (0-40 U/L)	25-80	24-85	33	74¶	27-225	20-62	36	24-61	27-35	34-207	38-52	42-61	115	34-42	27-126	36-55	18-58	26-57	23-30	33-237	24-74	39-47	526	
CPK (0-174 U/L)	75-201	73-226	159	7-69	55-157	241-1351	689-828	267-318	71-91	375-1041	180-313	102-183	104	54	121-150	121	125-2684	104-644	36-196	382	N/A	115	86	
Vitamin B12 (193-982 pg/mL)	N/A	316	926	518	670	N/A	N/A	N/A	966	573	N/A	540	907	455	N/A	626	N/A	N/A	N/A	617	N/A	N/A	156	
Serum magnesium (0.66-1.07 mmol/L)§	0.69-0.97	0.67-1	0.82	0.74-1.07	0.56-0.8†	0.81-0.86	0.86-0.87	0.86-0.9	0.8-0.88	0.85-1.01	0.86-0.89	0.88	0.83	0.83-0.88	0.76-0.82	0.78-0.92	0.77-0.98	0.72-0.86	0.99	N/A	N/A	0.85-0.86	0.89 mmol/L	
Ionized magnesium (0.44-0.59 mmol/L)§	0.49	0.55	0.58	N/A	0.4-0.57†	0.46-0.49	0.55	0.55	0.52-0.53	0.48-0.7	0.53	0.51	0.51	0.51	0.47	0.49-0.52	0.51-0.56	N/A	0.52	N/A	N/A	0.57	N/A	
RICD	Impaired	Impaired	Impaired	N/A	Impaired	Normal	Impaired	Impaired	Impaired	Impaired	Normal	N/A	N/A	N/A	N/A	N/A	N/A	N/A	Impaired	N/A	N/A	Impaired	N/A	
Fas-Kill assay	Normal	Normal	Normal	N/A	Normal	Normal	Normal	Normal	Normal	Normal	Normal	N/A	N/A	N/A	N/A	N/A	N/A	N/A	Normal	N/A	N/A	Normal	Normal	

Units and where appropriate reference ranges are shown in parenthesis. * Includes values on Ig replacement therapy. † Calculated from copies/mL. ‡ Patient on chemotherapy. § Prior to Mg2+ supplementation. ¶ Patient with diabetes insipidus, includes values on magnesium supplementation. ¶ Prior to starting chemotherapy for lymphoma and HSCT. ** Lowest value. †† Diagnosed post-mortem.

Supplementary Table 3: Genotypes of XMEN patients

<i>MAGT1</i> Mutation	Family (patients)
c.859_997del139, p.N287X	A (1-3)*, F(1,2)*
c.409C>T, p.R137X	B (1), D (1), L (1,2), O (1)
c.236G>A, p.W79X	C (1)
c.598_598delC, p.R200GfsX13	E (1)
c.774_774delT, p.F258LfsX5	G (1,2)
c.991C>T, p.R331X	H (1)
c.712C>T, R238X	I (1,2)
c.110G>A, p.W37X	J (1,2)
Partial gene deletion exons 3-10	K (1,2)
c.901-902insAA, p.T301KfsX14	M (1,2)
Partial gene deletion introns 1-8	N (1)
c.223C>T, p.Q75X	P(1)
c.414C>A, p.Y138X	Q(1)
c.555dup, p.Y186IfsX2	R(1) †

MAGT1 NCBI Reference Sequence: NM_032121.5. Patients are listed according to their family letter, followed by their patient number (Patient A-1, Patient B-1, etc.). *Families A and F have different genomic mutations, but they both result in the same c.DNA and protein alterations (Family A:g.46668_46677del 10, Family F: g.46604G>T). †Reference (1).

Supplementary table 4: Liver disease in XMEN

Patient	EBV in blood	EBER	Transfusions (PRBCs)	Hemosiderin deposits in liver	Hepatosteatosi s	Ballooning injury	Inflammation pattern	CK7	Fibrosis	Other
B.1	Positive	N/A	Yes	Yes	Yes	No	N/A	Yes	Periportal	Congestion + periportal fibrosis; cholangiolar, hepatocellular, cannicular cholestasis.
A.1	Positive	Negative	No	No	Minimal	No	Portal + Lobular	No	No	
I.2	Positive	Negative	Yes	Mild hepatocellular (zone 2 + 3), moderate reticuloendothelial.		No	None	N/A	No	
D.1	Positive	N/A	Yes	No	Moderate	Prominent	Foci of lobular; mid portal - associated with mild focal piecemeal-like necrosis	N/A	Bridging	Marked glycogenosis. Comorbidity: morbid obesity.
L.1	Negative	Negative	No	N/A	No	No	Minimal: portal and sinusoidal along zone 1	N/A	Mild peri-portal - lymphocytes and macrophages	Diffuse glycogenosis.
O.1	Positive	N/A	Yes	No	Minimal	No	Minimal: portal areas; rare lobular.	No	Peri-portal trapping and mild ductular reaction	
Q.1*	Positive	N/A	No	Hepatocytes and kupffer cells	No	No	N/A	N/A	None	
R.1†	Positive	N/A	Yes	N/A	Moderate	Prominent	Rare foci of lobular inflammation. Mild portal chronic inflammatory infiltrate associated with mild, focal piecemeal-like necrosis.	N/A	Bridging	No Mallory bodies and negative for ubiquitin.

PRBCs: packed red blood cells. *Biopsy specimen not available at NIH (outside report). †NIH pathology report of previously published case (1).

Supplementary Table 5: Non-malignant lymphoid histopathological findings

Patient	Tissue	EBER	Pathology
A.1	Tonsils and adenoids	+	Follicular hyperplasia with increased number of EBV-positive cells.
D.1	Cervical and inguinal lymph nodes	+	Follicular hyperplasia and Inguinal atypical lymphoid proliferation.
G.2	Inguinal lymph node	+	Reactive lymphoid hyperplasia and increased cells positive for Epstein-Barr virus.
	Small intestinal mucosa	+	Terminal ileum mucosa with reactive mucosal lymphoid follicles.
J.2	Cervical lymph node	-	Reactive lymphoid hyperplasia with Castleman changes and focal follicular lysis.
	Adenoids	-	Reactive lymphoid hyperplasia
P.1	Mediastinal mass	-	Atypical lymphoid tissue comprised of small lymphocytes, and scattered histiocytes/dendritic cells with a polyclonal TCR/BCR rearrangement.

Supplementary Table 6: Cancer Predisposition in XMEN disease

ID	Age at cancer diagnosis	Current age	Type	EBV viremia	EBER (tumor)
B.1	45	45†	Lymphoma	+	N/A
D.1	12	20†	EBV-positive LPD of the hypothalamus*	+	+
F.1	17, 22	23†	Classical Hodgkin lymphoma	+	N/A
E.1	7, 13	22	Burkitt's lymphoma	+	+
I.2	13	31	EBV-positive LPD of the palate*	+	+
	27		Liposarcoma		-
I.1(2)	57	57	Diffuse large B-cell lymphoma	+	N/A
K.2	15	15	Classical Hodgkin lymphoma	+	+
M.2*	16	18	EBV-positive LPD*	+	+
N.1	29	49	Classical Hodgkin lymphoma	+	N/A
R.1 (1)	15	18†	Classical Hodgkin lymphoma	+	-
Ref.(3)	5	N/A	Kaposi sarcoma	+	N/A

N/A not available. *Given the severity of the disease EBV-positive lymphoproliferative disease (LPD) is included in this table. † Age at death. Reference (Ref.).

Supplementary Table 7: Mass cytometry staining panel

Metal	Epitope	Clone	Serial #	Lot #
089Y	CD45	HI30	3089003B	2291710
116Cd	CD70-Biotin & Streptavidin-Qdot 655	113-16	355114 & Q10121MP	NA
141Pr	CD196 (CCR6)	G034E3	3141003A	831717
143Nd	HLA-DR	L243	3143013B	1711719
144Nd	CD31	WM59	3143013B	1711719
145Nd	CD4	RPA-T4	3145001B	3391705
146Nd	CD8	RPA-T8	3146001B	1671716
147Sm	CD20	2H7	3147001B	3081607
148Nd	IgA	Polyclonal	3148007B	2481401
149Sm	CD56	NCAM16.2	3149021B	3331703
151Eu	CD14	M5E2	3151009B	2351604
152Sm	TCR $\gamma\delta$	11F2	3152008B	1531708
153Eu	CD62L	DREG-56	3153004B	1351720
154Sm	CD3	UCHT1	3154003B	1351723
155Gd	CD27	L128	3155001B	1031712
156Gd	CD184/CXCR4	12G5	3156029B	471708
158Gd	CD10	HI10a	3158011B	1131612
159Tb	CD22	HIB22	3159005B	3001407
162Dy	CD11c	Bu15	3162005B	1671707
163Dy	CD57	HCD57	3163022B	2671603
164Dy	CD161	HP-3G10	3164009B	3271610
165Ho	CD45RO	UCHL1	3165011B	1421721
166Er	CD314/NKG2D	ON72	3166016B	91703
167Er	CD38	HIT2	3167001B	1731804
169Tm	CD25	2A3	3169003B	1931713
170Er	CD45RA	HI100	3170010B	3521705
171Yb	CD185/CXCR5	51505	3171006B	471707
172Yb	IgM	MHM-88	3172004B	1671708
174Yb	CD94	HP-3D9	3174015B	2181508
175Lu	CD279/PD-1	EH12.2H7	3175017B	3391708
176Yb	CD127	A019D5	3176008B	1671712
191Ir	DNA1	-	201192A	NA
193Ir	DNA2	-	201192A	NA
195Pt	Cisplatin	-	201198	NA
209Bi	CD11b	ICRF44	3209003B	831723

All metal-tagged reagents were from Fluidigm, the biotinylated anti-human CD70 antibody was from BioLegend, and the Qdot-655 Streptavidin Conjugate was from Thermo Fisher.

Supplementary Table 8: Abnormally glycosylated proteins in XMEN

Overglycosylated Proteins

Protein ID	Protein Name	Function	Diseases
EMB*	Embiggin	Transmembrane glycoprotein, of the immunoglobulin superfamily, involved in motoneuron outgrowth and formation of neuromuscular junctions. This is a putative chaperone for the cell surface transporter MCT2 DOI: 10.1074/jbc.M411950200	No known diseases
SLC1A4*	Neutral Amino Acid Transporter (Solute Carrier Family 1 Member 4)	Sodium dependent transporter of serine, cysteine, threonine and alanine	Spastic tetraplegia, thin corpus callosum, and progressive microcephaly https://doi.org/10.1111/cge.12605
HLA-DQB1*	Major Histocompatibility Complex, Class II, DQ Beta-1	Binds peptides derived from endocytosed antigens. Presents antigen peptides on surface of cell for CD4 T cell recognition.	Celiac disease (susceptibility to) https://doi.org/10.1086/338453 Variant Creutzfeldt-Jakob Disease (resistance to) https://doi.org/10.1038/35104694 Multiple sclerosis (susceptibility to) https://doi.org/10.1093/hmg/7.8.1235
SLC12A2*	Sodium/Potassium/Chloride Transporter (Solute Carrier Family 12, Member 2)	Electrically silent transporter system. Mediates sodium and chloride reabsorption. Plays a vital role in the regulation of ionic balance and cell volume.	No known diseases
CEACAM1	Carcinoembryonic Antigen-Related Cell Adhesion Molecule 1	Cell adhesion protein that mediates homophilic cell adhesion in a calcium independent manner	Linked to insulin uptake in obesity and non-alcoholic fatty liver disease. https://doi.org/10.3389/fendo.2017.00008
CEACAM6	Carcinoembryonic Antigen-Related Cell Adhesion Molecule 6	Cell surface glycoprotein involved in cell adhesion and tumor progression	No known diseases
TSPAN31*	Tetraspanin 31	Also known as a Sarcoma Amplified Sequence (SAS). Family of proteins that are transmembrane with tumor-associated and hematopoietic cell proteins	No known diseases
SPPL2A	Signal Peptide Peptidase-Like 2A	Intramembrane cleaving aspartate protease which functions in CD74, FASLG, ITM2B and TNF processing	Susceptibility to mycobacterial disease https://doi.org/10.1038/s41590-018-0178-z
ICAM3	Intercellular Adhesion Molecule 3	Leukocyte adhesion molecule that binds LFA-1, integrin alpha-D/beta-2 and contributes to apoptotic neutrophil phagocytosis by macrophages	No known diseases
C10orf54	V-type Immunoglobulin Domain-Containing Suppressor of T-Cell Activation	Receptor involved in inhibition of T-cell response	No known diseases
ITGAM	Integrin Alpha-M	Used in adhesion of monocytes, macrophages and granulocytes, as well as the uptake of complement-coated particles	Systemic lupus erythematosus (association with susceptibility to) https://doi.org/10.1093/hmg/ddp118
CD101	Immunoglobulin Superfamily Member	Inhibits T-cell proliferation induced by CD3 through inhibition of IL2 and expression of IL2RA on activated T-cells	Point mutations increase susceptibility to Type 1 Diabetes https://dx.doi.org/10.1111%2Fjdi.12586 and increased risk of HIV infection https://dx.doi.org/10.1371%2Fjournal.ppat.1006703
TMEM87A*	Transmembrane Protein 87A	Retrograde transport from endosomes to trans-Golgi network	No known diseases
PKD2	Polycystin 2	Cation channel in fluid-flow mechanosensation of primary cilium of renal epithelium. K+ channel with Ca+2 permeability and limited Na+ permeability	Polycystic kidney disease 2 http://dx.doi.org/10.1126/science.272.5266.1339
ITGA5	Integrin Alpha-5	Receptor for fibronectin and fibrinogen; involved in cell adhesion.	No known diseases
P2RY10	Putative P2Y Purinoceptor 10	Receptor for G-protein coupled purines	No known diseases

Underglycosylated Proteins

Protein ID	Protein Name	Function	Diseases
GPR171	Probable G Protein-Coupled Receptor 171	Orphan receptor	No known diseases
HLA-E	HLA Class I Histocompatibility Antigen, Alpha Chain E	Binds signal sequences of HLA-A, -B, -C and -G molecules	Association with type 1 diabetes, Behcet's disease and pemphigus vulgaris https://doi.org/10.1111/exd.12077
CLAR	Calreticulin	Calcium binding chaperon in the endoplasmic reticulum; involved in maternal gene expression regulation	Myelofibrosis (somatic) and Thrombocytopenia (somatic) https://doi.org/10.1056/NEJMoa1311347
CERS5	Ceramide Synthase 5	Dihydroceramide synthase that catalyzes the acylation of sphingosine to form dihydroceramide	No known diseases
ST3GAL1	CMP-N-Acetylanneuraminate-Beta-Galactosamide-Alpha-2,3-Sialtransferase 1	Synthesizes the sequence found on sugar chains O-linked to threonine and serine and as the terminal sequence on some gangliosides	No known diseases
SLCO3A1	Solute Carrier Organic Anion Transporter Family Member 3A1	Na+ independent transporter of prostaglandins E1 and E2, thyroxine, deltrophin II, BQ-123 and vasopressin	No known diseases
RCN1	Reticulocalbin 1	Regulates calcium dependent activities in the ER lumen/post-ER compartment	No known diseases
HSP90B1	Endoplasmic (Heat Shock Protein 90)	Molecular chaperone that is involved in proper folding of Toll-like receptors	No known diseases
MAN2A1	Alpha Mannosidase 2	Catalyzes the commitment step in the biosynthesis of complex N-glycans	Contributes to inflammatory bowel disease https://doi.org/10.1247/csf.17022
TM2D1	TM2 Domain-Containing Protein 1	Participates in amyloid-beta-induced apoptosis	No known diseases
SLC7A1	High Affinity Cationic Amino Acid Transporter 1	Transporter of cationic amino acids in non-hepatic tissues	No known diseases
ATG9A	Autophagy-Related Protein 9A	Functions in autophagy and cytoplasm to vacuole transport vesicle formation	ATG9A shows immunoreactivity in ALS-like mice https://doi.org/10.5115/acb.2014.47.2.101
CD28	T-Cell-Specific Surface Glycoprotein CD28	T-cell activation, cell proliferation, cytokine production, especially IL4 and IL10, and promotion of T-cell survival	Mutations can contribute to T cell lymphomas https://doi.org/10.1016/j.celim.2017.07.002
KLRK1	NKG2-D Type II Integral Membrane Protein	Activating and costimulatory receptor involved in immunosurveillance which acts on NK cells and TCR in CD8+ T-cells	No known diseases

CD6	T-cell Differentiation Antigen CD6	Cell adhesion molecule that regulates T-cell responses through mediation of cell-cell contacts	No known diseases
EDEM1	ER Degradation-Enhancing Alpha-Mannosidase-Like Protein 1	Targets degradation of misfolded glycoproteins from the calnexin cycle in the endoplasmic reticulum	No known diseases
CDS2	Phosphatidate Cytidyltransferase 2	Synthesizes CDP-diacylglycerol, an important precursor to phospholipids	No known diseases
ALG9	Alpha-1,2-Mannosyltransferase ALG 9	Catalyzes the transfer of mannose to lipid-linked oligosaccharides	Congenital disorder of glycosylation (type II) https://doi.org/10.1086/422367 Gillesen-Kaesbach-Nishimura syndrome https://doi.org/10.1038/ejhg.2015.91
TRAC	T Cell Receptor Alpha Constant	Constant region of alpha chain of T cell receptor	Immunodeficiency 7 (TCR-alpha/beta deficient) https://doi.org/10.1172/JC141931
PON2	Serum Paraoxonase/Arylesterase 2	Hydrolyzes lactones and aromatic carboxylic acid esters and reduces mildly oxidized LDL	Coronary artery disease (susceptibility to) https://doi.org/10.1086/301669
CIGALTIC1	CIGALT1-Specific Chaperone 1	Chaperone for CIGALT1 that is required for generation of a common O-glycan precursor	Tn polyagglutination syndrome (somatic) https://doi.org/10.1038/4371252a
PLAUR	Urokinase Plasminogen Activator Surface Receptor	Localizes and promotes plasmin formation by signal transduction of U-PA	Linked to polyautoimmunity https://doi.org/10.1016/j.jaut.2016.05.003
LY75	Lymphocyte Antigen 75	Endocytic receptor that directs captured antigens from the extracellular space; reduces proliferation of B lymphocytes	Association to inflammatory bowel disease https://doi.org/10.1155/2016/6485343
P2RY8	P2Y Purinoceptor 8	Receptor of purines coupled to G-proteins	Association with B cell lymphomas https://doi.org/10.1016/j.jimolx.2016.03.004
SLC4A7	Sodium Bicarbonate Cotransporter 3	Regulates intracellular pH through co-transporting sodium and bicarbonate	Associated with hypertension https://doi.org/10.1093/hmg/ddu478
ERMP1	Endoplasmic Reticulum Metallopeptidase 1	Organization of somatic cells and oocytes in ovaries	No known diseases
TPST2	Protein-Tyrosine Sulfoxtransferase 2	Catalyzes O-sulfation of tyrosine residues	No known diseases
ANO9	Anoctamin 9	Calcium dependent scramblase	No known diseases
PIIB	Peptidyl-Prolyl cis-trans Isomerase B	Assists protein folding by isomerizing proline imidic peptide bonds	Osteogenesis imperfecta (type IX) https://doi.org/10.1093/hmg/ddr037
CHST11	Carbohydrate Sulfoxtransferase 11	Adds sulfate to chondroitin, the predominant proteoglycan in cartilage	In frame 15nt deletion caused hand/foot malformation and malignant lymphoproliferative disease http://dx.doi.org/10.1136/jmedgenet-2017-105003 SNPs linked to osteoarthritis https://doi.org/10.1371/journal.pone.0159024
ASAH1	Acid Ceramidase	Hydrolyzes sphingolipid ceramide	Farber lipogranulomatosis https://doi.org/10.1074/jbc.271.51.33110 Spinal muscular atrophy with progressive myoclonic epilepsy https://doi.org/10.1016/j.ajhg.2012.05.001
GPR55	G-Protein Coupled Receptor 55	Receptor for L-alpha-lysophosphatidylinositol, triggering Ca ²⁺ release and playing a role in hyperplasia associated with inflammation and neuropathic pain	Knockout in mice leads to age-related ventricular dysfunction and impaired adrenoceptor-mediated inotropic responses https://doi.org/10.1371/journal.pone.0108999
LMBRD1	Probable Lysosomal Cobalamin Transporter	Exports cobalamin from lysosomes	Methylmalonic aciduria and homocystinuria (cblF type) https://doi.org/10.1038/ng.294
SLC12A9	Solute Carrier Family 12 Member 9	Inhibitor of SLC12A1, a sodium and chloride transporter	No known diseases
LNPEP	Leucyl-Cystinyl Aminopeptidase	Degrades oxytocin, vasopressin and angiotensin and may inactivate neural proteins in the brain	Association with psoriasis https://doi.org/10.1038/jid.2013.317 And autism https://doi.org/10.1007/s12264-017-0120-7
GDPD5	Glycerophosphodiester Phosphodiesterase Domain-Containing Protein 5	Promotes differentiation of motor neurons	No known diseases
PTGER4	Prostaglandin E2 Receptor EP4 Subtype	Receptor for prostaglandin E2 coupled to G-proteins that relaxes smooth muscle	Associated with Crohn's disease https://doi.org/10.1007/s00384-014-1881-3
IL17RA	Interleukin-17 Receptor A	Receptor of IL-17 which induces proinflammatory cytokine expression	Immunodeficiency 51 https://dx.doi.org/10.1126%2Fscience.1200439
ITPR2	Inositol 1,4,5-Triphosphate Receptor Type 2	Involved in the release of intracellular calcium via inositol 1,4,5-triphosphate signaling	Anhidrosis (isolated, with normal sweat glands) https://doi.org/10.1172/JC120720
CLCN5	H(+)/Cl(-) Exchange Transporter 5	Antiporter involved in the acidification of the endosome lumen	Dent disease, Hypophosphatemic rickets and Nephrolithiasis (type I) https://doi.org/10.1038/379445a0 Proteinuria (low molecular weight, with hypercalcaemic nephrocalcinosis) https://doi.org/10.1172/JC1119262
TMEM181	Transmembrane Protein 181	G-protein coupled receptor that responds to cytolethal distending toxin from bacteria	Association with dental caries https://doi.org/10.1186/s12903-018-0559-6
CLEC2B	C-Type Lectin Domain Family 2 Member B	Initiates cross talk between myeloid and NK cells through NKp80 binding, and is involved in the activation of platelets	CLEC2B deletion causes lymphatic insufficiency in mice https://doi.org/10.1182/blood-2016-04-636415
CERS2	Ceramide Synthase	Synthesize sphingolipids	Deletion aggravates colitis in mice https://doi.org/10.1007/s00018-017-2518-9
PLXNA3	Plexin 3A	Receptor for signaling that regulates cytoskeletal morphology and plays a role in axon guidance in developing neurons	Association with multiple sclerosis https://doi.org/10.1007/s12017-017-8443-0
SIPR4	Sphingosine 1-Phosphate Receptor 4	Receptor for sphingosine 1-phosphate (S1P), which is involved in cell migration of lymphocytes	No known diseases
PTGDR2	Prostaglandin D2 Receptor 2	G-Protein Coupled Receptor whose activation mediates immune regulation and inflammatory response	No known diseases
LGALS3BP	Galectin-3-Binding Protein	Promotes cell adhesion through integrin	No known diseases
NPC1	NPC Intracellular Cholesterol Transporter 1	Exports cholesterol from the endosomal/lysosomal compartment to the ER and plasma membrane	Niemann-Pick disease (type C1 and type D) http://dx.doi.org/10.1126/science.277.5323.228
SLC23A2	Solute Carrier Family 23 Member 2	Sodium and Ascorbate (Vitamin C) cotransporter	No known diseases
ABCA2	ATP-Binding Cassette Sub-Family A Member 2	Probable transporter in macrophage lipid metabolism and neural development	Association with Alzheimer's Disease https://doi.org/10.1016/j.nbd.2004.09.011
GALNT4	Polypeptide N-Acetylgalactosaminyltransferase 4	Catalyzes a step in O-linked oligosaccharide biosynthesis	No known diseases
B4GALT3	Beta-1,4-Galactosyltransferase 3	Responsible for N-linked oligosaccharide synthesis for many glycoproteins	A potential association to Hutchinson-Gilford Progeria https://doi.org/10.1002/ajmg.10753
JMJD8	JmjC Domain Containing Protein 8	No known function	No known diseases

CLEC12A	C-Type Lectin Domain Family 12 Member A	Receptor involved in signaling cascades, especially involving MAP kinases	No known diseases
SYPL1	Synaptophysin-Like Protein 1	Maintenance of vesicle structure	No known diseases
GPR112	Adhesion G-Protein Receptor G4	Orphan receptor	No known diseases
SLC22A5	Solute Carrier Family 22 Member 5	Sodium carnitine cotransporter	Carnitine deficiency (systemic primary) https://doi.org/10.1038/5030

* Peptides are both overglycosylated and underglycosylated, at different sites.

Information was found using the UniProt database (<https://www.uniprot.org/>), the Online Mendelian Inheritance in Man (OMIM) database (<https://www.omim.org/>), and PubMed (<https://www.ncbi.nlm.nih.gov/pubmed/>).

Supplementary Table 9: Transferrin and apolipoprotein CIII isoform analysis

Transferrin*	Normal range	A.1	A.2	A.3	E.1	H1	J.1	L.1	L.2	N1	Q.1
Mono-Oligosaccharide/Di-Oligosaccharide	≤ 0.06	0.18	0.16	0.14	0.18	0.17	0.16	0.16	0.16	0.13	0.15
A-Oligosaccharide /Di-Oligosaccharide	≤ 0.011	0.005	0.009	0.008	0.006	0.003	0.004	0.005	0.005	0.12	0.009
Tri-sialo/Di-Oligosaccharide	≤ 0.05	0.05	0.06	0.06	0.03	0.06	0.05	0.04	0.08	0.05	0.06
Apolipoprotein CIII**											
Apo CIII-1/CIII-2	≤ 2.9	3.33	2.63	2.19	2.43	2.69	2.11	2.20	4.52	1.61	1.72
Apo CIII-0/Apo CIII-2	≤ 0.48	1.01	0.8	0.39	0.34	0.66	0.75	0.52	0.78	0.17	0.33

* Mass spectrometry; reflects N-linked glycosylation

**Reflects O-linked glycosylation

Supplementary Table 10: Comparison of XMEN and ALPS

	XMEN	ALPS-FAS
Clinical findings		
Sex	Male	Male/Female
Non-malignant lymphadenopathy and/or splenomegaly	Mild/moderate	Significant
Autoimmune cytopenias	May be present	Frequent
Recurrent sinopulmonary infections	Yes	No
Severe molluscum contagiosum	Common	May be seen with immunosuppressive treatment
Family history	Maternal male relatives	Positive except for ALPS-sFAS
Increased susceptibility to lymphoma	Predominantly EBV+	Hodgkin and non-Hodgkin lymphoma
Serum Ig	Normal or Low IgA and IgG	High
Lymphocyte subsets		
NKG2D	Low	Normal
B cells	Elevated	Normal
CD4/CD8 ratio	Low	Normal
alpha-beta DNT cells	High	High
CD45R(B220) ⁺ αβ DNT cells	Normal	High
Persistent EBV viremia	Yes (except for EBV-naïve individuals)	Rare
Biomarkers		
sFasL	Predominantly Low/normal	High (>200 pg/mL)
IL-10	Variable	High (>20 pg/mL)
IL-18	Variable	High (>500 pg/mL)
Vitamin B12	Normal	High (>1500 ng/L)
Elevated liver transaminases	Yes	No (except in case of autoimmune hepatitis)
CPK	High/normal	Normal
Functional assays		
Defective FAS apoptosis	No	Yes
Defective RICD	Yes	Yes (mild)
Genetics		
Affected gene	<i>MAGT1</i>	<i>FAS</i> (germline or somatic)*
Inheritance	X-linked	Autosomal dominant with incomplete penetrance. Rarely, autosomal recessive due to heterozygous or homozygous mutations.

*Mutations in genes encoding *FASL*, *FADD*, and *CASP10* also cause ALPS termed ALPS-FASL, ALPS-FADD, and ALPS-CASP10, respectively (not discussed here).

References

1. Patiroglu T, Haluk Akar H, Gilmour K, Unal E, Akif Ozdemir M, Bibi S, et al. A case of XMEN syndrome presented with severe auto-immune disorders mimicking autoimmune lymphoproliferative disease. *Clin Immunol.* 2015;159(1):58-62.
2. Dhalla F, Murray S, Sadler R, Chaigne-Delalande B, Sadaoka T, Soilleux E, et al. Identification of a novel mutation in MAGT1 and progressive multifocal leucoencephalopathy in a 58-year-old man with XMEN disease. *J Clin Immunol.* 2015;35(2):112-8.
3. Brigida I, Chiriaco M, Di Cesare S, Cittaro D, Di Matteo G, Giannelli S, et al. Large Deletion of MAGT1 Gene in a Patient with Classic Kaposi Sarcoma, CD4 Lymphopenia, and EBV Infection. *J Clin Immunol.* 2017;37(1):32-5.